Int J Adv Manuf Technol (2011) 54:1043–1055
DOI 10.1007/s00170-010-3016-5

ORIGINAL ARTICLE

Fabrication of copper/aluminum composite tubes by spin-bonding process: experiments and modeling

Mohammad Sadegh Mohebbi · Abbas Akbarzadeh

Received: 4 April 2010 / Accepted: 1 November 2010 / Published online: 11 November 2010

Abstract The aim of this work is to produce two layered thin-walled Cu/Al composite tube by the spin-bonding process. The process is utilized to bond the aluminum tube into the copper one at thickness reductions of 20–60% and process temperatures of 25°C, 130°C, and 230°C. The bond strength is measured by T-peeling test, and the bond interfaces are examined by metallography and scanning electron microscopy (SEM). The results show that after a threshold thickness reduction of about 30%, the bond strength increased with the amount of deformation. SEM fractography of the peel surfaces confirms that the copper oxide film is broken in a shear manner during deformation. Severe shear strains applied during spin-bonding process, in fact, make it appropriate for bonding the copper to aluminum. Based on the results, at higher temperatures the resulted bond strength is decreased. It is shown that formation of the brittle intermetallic layer on the interface at high temperatures leads to decrease in the bond strength. In addition to the experiments, a procedure is proposed by which it is possible to calculate the bonding length through the comparison of FEM simulations and the experiments. Based on these calculations and the bonding mechanism, a bond strength model is developed and verified by the experiments.

Keywords Spin bonding (SB) · Cold bonding · Tube spinning · Cu/Al composite tube · FEM analysis · Modeling

M. S. Mohebbi · A. Akbarzadeh (✉)
Department of Materials Science and Engineering,
Sharif University of Technology,
Azadi Ave., P.O. Box 11155-9466, Tehran, Iran
e-mail: abbasa@sharif.edu

M. S. Mohebbi
e-mail: msmohebi@mehr.sharif.edu

Nomenclature

α	Roller attack angle
f	Feed rate
r	Thickness reduction
D	Mandrel diameter
T	Thickness of the tubes
T'	Thickness of tubes obtained by the FEM simulations
l_b	Bonding length
L	Axial length of the deformation zone
A	Surface of the tubes
f_A	Surface fraction of the virgin metals
f_{A_c}	Surface fraction of correlated contact of the virgin metals
S_b	Bond strength

Subscripts

r, θ, z	Radial, circumferential, and axial directions
i, e	Internal and external layers
$0, b, f$	Initial, bonding, and final sections

Superscripts

I, II	After and before bonding section

1 Introduction

Clad metals, consisting of two or more metals, are increasingly used in many industries because of their unique properties. They have material properties that cannot be obtained from a single material. Enhanced mechanical properties, corrosion resistance, electrical conductivity, fatigue characteristics, and wear resistance are the main industrial demands that can be met in this way [1–3]. Roll bonding is the most common cladding process used in manufacturing of the clad sheets and metal laminates. The

process consists of rolling two different metals together followed by a annealing heat treatment to enhance the bond strength by complex interface phase development [4].

Roll bonding of Cu/Al has been studied by several researchers, most of them have focused on the formation of intermetallic phases on the interface in annealing time and their effects on the bond strength [1, 2, 4–8]. The results of roll bonding of Cu/Al at high temperatures followed by annealing indicate that there are optimum values of annealing time and temperature and process temperature by which the most appropriate bond strength is achieved [1, 6, 7]. It has also been reported that roll bonding of Cu/Al at room temperature followed by annealing at 250°C for various times show no optimum conditions for annealing, so that the bond strength is reduced by annealing time [2]. From the welding point of view, aluminum and copper are incompatible metals because they have a high affinity to each other at temperatures higher than 120°C and produce brittle and low strength intermetallics. Thus, fusion-welding processes are not applicable for Cu/Al welding and solid-state welding processes such as explosion, friction, and cold roll welding have been considered as the qualified welding processes of these metals [2].

Circular-shaped hollow sections like tubes and cylinders, as the extensively used category of engineering components, are also expected to be clad. In many cases, their inner and outer surfaces are exposed to different environments, so that, different characteristics are required at inside and outside. Various bimetallic or clad tubes are utilized in boilers, heat exchangers, nuclear power plants, petroleum, and chemical industries [9]. Although it is possible to fabricate seamy clad tubes by roll-bonded clad sheets, it is ideal to plan a method with advantages of roll bonding to produce seamless thin-walled tubes and cylinders. So far, several methods have been used to produce clad and composite tubes. While extrusion [9, 10] can be used to fabricate the thick-walled bimetallic tubes, explosive bonding [11], ball attrition [3], hydraulic expansion method [12] are capable of manufacturing thin-walled cylinders. Recently, based on flow-forming process, a novel bonding process entitled as spin bonding is proposed by the authors to produce seamless thin-walled clad tubes and cylinders [13]. Flow forming or tube spinning is a forming process to produce thin-walled high-precision tubular components. In this process, a thick-walled workpiece fits on a rotating mandrel while one or more rollers, which have a degree of freedom about their own axes, move axially along the workpiece axis to reduce its thickness [14]. Using two fitted tubes on each other after surface treatment as the workpiece, it is possible to bond them by applying thickness reduction in tube-spinning process. In this work, spin-bonding process is used to bond the aluminum tube into the copper one at various thickness reductions and process temperatures. A model for spin bonding is also developed to calculate the bonding length and the bond strength.

2 Experimental methods

Commercially pure copper and aluminum after annealing were used in this study. Thickness of the internal and external tubes was 1 and 0.82 mm, respectively. The inner diameter of the internal tube (aluminum) was 51 mm, and the external tube (copper) was fitted on it. The bonding surfaces were degreased in acetone and scratch brushed with a 50 mm diameter steel circumferential brush of 0.35 mm wire diameter and surface speed of ~7 ms^{-1}. Then, the two tubes to be joined were positioned against each other. After that, a series of spin-bonding experiments were conducted applying 20% to 60% reductions in thickness. The time between surface preparation and spin bonding was kept to less than 300 s to avoid formation of the contaminant film and a thick oxide layer on the bond surfaces of the tubes. The process is schematically illustrated in Fig. 1a.

Spin-bonding process was carried out on a common lathe (Fig. 1b). A single roller tool was designed and built to accommodate the lathe tool post. The mandrel was clamped into the chuck of the lathe. Dimensions of the tools and the process conditions are given in Table 1.

In order to study the temperature effect on the Cu/Al bond strength, spin bonding was carried out at three different temperatures of 25°C, 130°C, and 230°C. A thermal element (Fig. 1c), slip ring, and brush-holder system was utilized to heat up the mandrel and workpiece during the spin-bonding process. The slip ring was mounted on the end of the shaft of lathe and the brush holder was fitted on it to have electrical connection. Electrical wires were passed through the shaft to the mandrel. While the slip ring was rotating with the shaft, two rings were used to monitor the mandrel temperature by a thermocouple fitted on its surface and two rings were to supply the electrical power for heating up the mandrel by the thermal element fitted into it (Fig. 1d).

The bond strength of the Cu/Al bimetal layers was measured by T-peeling test. Samples were 8 mm wide and 50 mm long and were cut at the longitude of the tubes so that their width was in the circumferential direction. A fixture was used during the test to fix the position of the rupture line and prevent the sample inclination from T-shape, Fig. 2. The breaking off force per width of the sample was measured as the bond strength (N/mm).

The bond interface of the longitudinal section of the spin-bonded tubes was examined by optical microscopy. After preparing these surfaces by standard metallographic

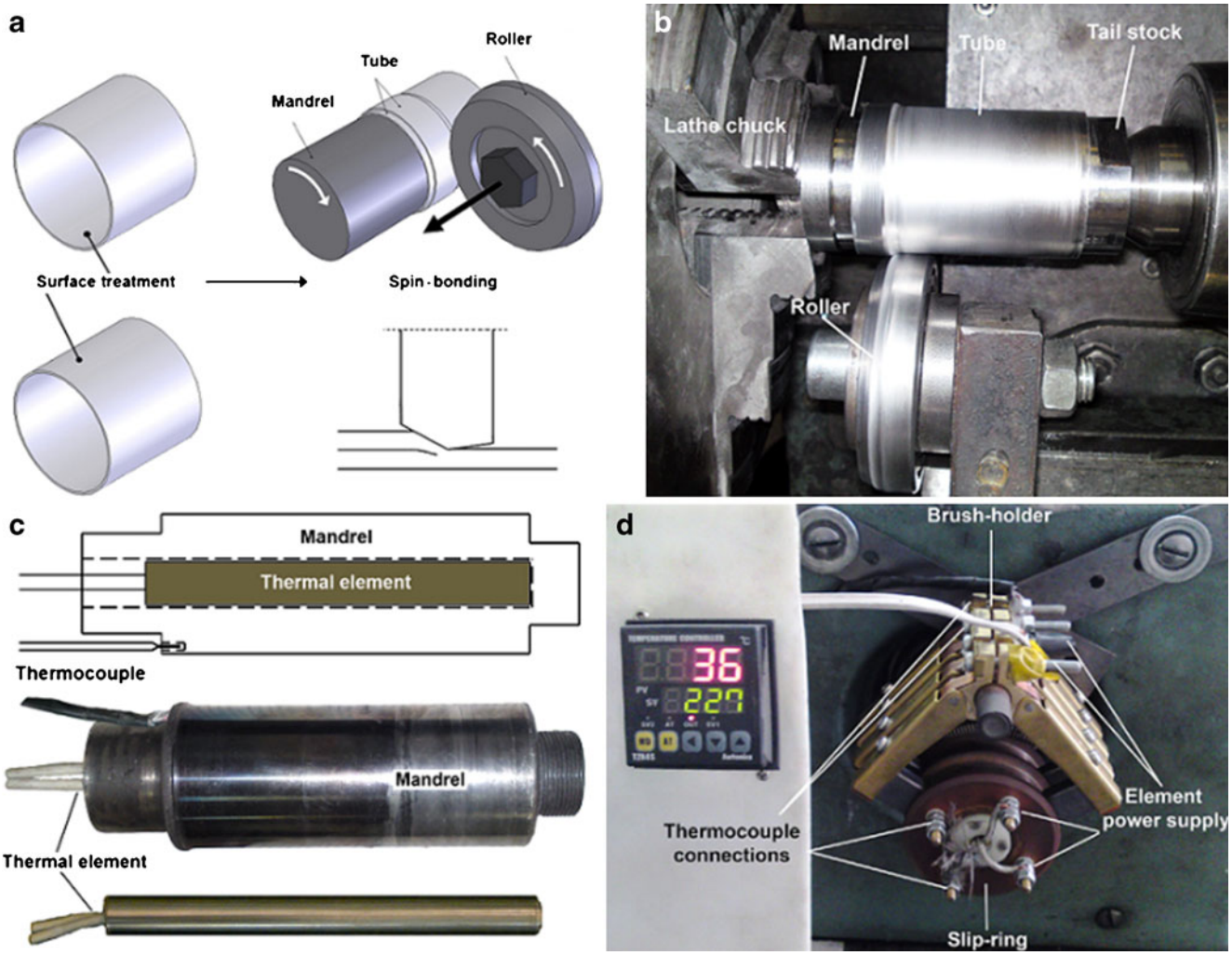

Fig. 1 **a** Schematic illustration of the spin-bonding, **b** tube-spinning set-up used for spin-bonding **c** thermal element and thermocouple and their positions in the mandrel, and **d** slip ring and brush-holder system

procedure as polished condition, chemical etching was performed to darken the possible intermetallic phases at interface. In this case, the specimens were exposed to 5 g picric acid in 100 ml ethanol for 15 min. To examine the efficiency of this solution, a successfully bonded specimen at ambient temperature was etched after annealing at 400°C for 30 min. Based on the previous studies, a thick layer of intermetallic phases is formed at the interface of Cu/Al under this annealing conditions [6].

A 15-kV scanning electron microscopy (SEM) with secondary electron detector was employed for fractography analysis. Fractography was done just after peeling to avoid any surface contamination and formation of a thick oxide layer. As brushed surfaces of the copper and aluminum tubes were also studied by SEM.

Table 1 Spin-bonding conditions

Parameter	Value
Temperature (K)	298, 400, 500
Reduction range (%)	20–60
Roller diameter (mm)	80
Roller attack angle (°)	17
Roller smooth angle (°)	3
Mandrel diameter (mm)	51
Feed rate (mm/rev.)	0.08
Speed of rotation (rpm)	500

3 FEM model

An elasto-plastic finite element method (FEM) analysis is utilized in this work for indirect calculation of the bonding length, l_b. Abaqus/Explicit commercial code was used to simulate the process. Wong et al. [15] have confirmed that the explicit FE code is ideal to tackle some issues in simulating the flow-forming process. Computational cost of

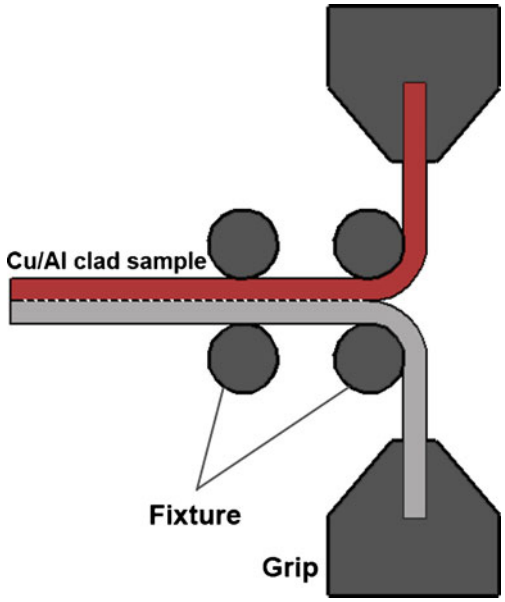

Fig. 2 Schematic illustration of the T-peel test

the simulation in the explicit procedure can be reduced by either speeding it up compared with the time of actual process or artificially increasing the material density by a factor called mass scaling. These deviations from the real conditions, however, have to be chosen in such an order that the inertia forces do not change drastically the predicted responses. In the present work, the mass scaling factor of 10^4 and the real time of 15 s for 1 cm advance of the roller by a feed rate of 0.08 mm/rev and rotational speed of 500 rev/min are chosen. The roller and the mandrel were modeled as rigid surfaces. As Wong et al. [15] have suggested, the workpiece and the mandrel were fixed and the roller was chosen to rotate about their axes. The roller appointed to rotate 785.4 rad (125 revolution) while it is traveling 10 mm in the axial direction to make a feed rate of 0.08 mm/rev.

Mohebbi and Akbarzadeh [13] have developed a FEM model for forward flow-forming process with three constraints by which the model size is decreased as close as possible to the real conditions. These constraints are utilized in the present model, as illustrated in the initial model set-up, Fig. 3. More details of the model as well as the validation of the results by experiments of tube spinning are available in that paper.

About 20,000 elements were distributed on the tubes. While three elements were appointed in the thickness of the tubes, half length of the tubes which did not undertakes the deformation was meshed with larger elements. All dimensions were similar to the experimental conditions (Table 1) except that the length of the tubes was 15 mm.

In order to compare the predicted results of the model with experimental ones, the process is simulated for four thickness reductions of 31%, 37%, 49%, and 61%. The elastic modulus of 130 and 70 GPa were respectively chosen for copper and aluminum tubes.

3.1 Contact conditions

Surface to surface contact with penalty formulation was used in this work. Bonding between the two layers was not assumed in the FEM analysis. As explained in section 5.1, the difference between the simulation and experimental results derived from this simplification is used for indirect calculation of the bonding length. However, friction between the tubes plays an important role in their deformation and has to be accurately determined and imposed in the FEM model. In this work, according to standard of ASTM G99, the coefficient of friction was determined as a function of normal pressure by a pin-on-disk tribometer set (Fig. 4). The pin and disk were prepared from pure copper and AA 1050, respectively, and then their surfaces were brushed under similar conditions of the tubes. Other conditions of the test are listed in Table 2. The test was carried out at various normal loads. During each test, the coefficient of friction was recorded by dividing the tangential load to the normal one. For example, the result for normal load of 1 kg is depicted in Fig. 5.

To calculate the normal pressure at each test it is necessary to know the contact area. Therefore, the apparent contact area after each test was measured by examining the wear track. The results are summarized in Fig. 6. It can be seen in this figure that the coefficient of friction is initially increased by the normal load, and then reaches to an almost

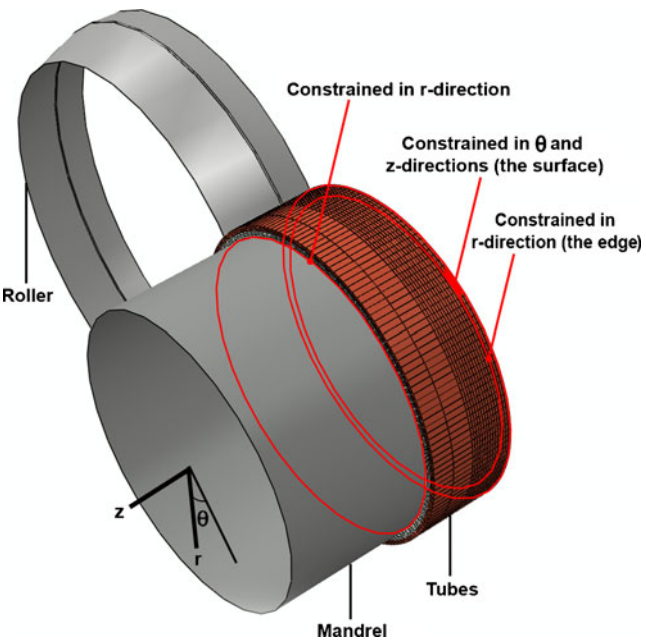

Fig. 3 The model used for FEM analysis

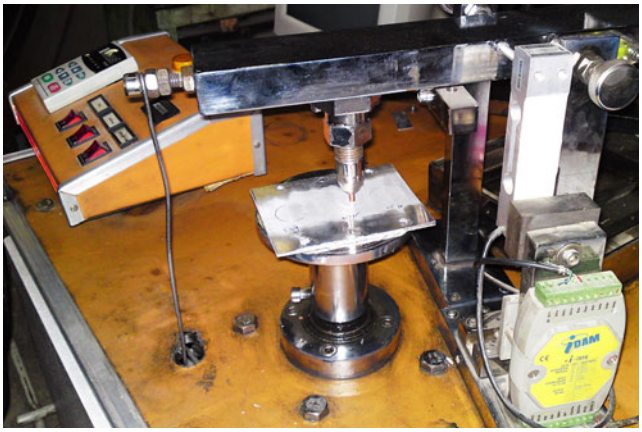

Fig. 4 The pin-on-disk tribometer set used for measurement of coefficient of friction

constant value which thereafter decreases by the normal load. Considering the measured apparent contact areas and normal loads, it is possible to calculate the normal pressure and determine the coefficient of friction as a function of normal pressure. The results are illustrated in Fig. 7. In this figure, the shear stress at each normal pressure is calculated by multiplying the related average of coefficient of friction to the normal pressure. It can be said that the decrease of coefficient of friction after normal pressure of 42 MPa is due to the fact that the shear stress reaches the values near to the shear strength of the aluminum disk and does not increase any more. The average coefficients of friction at normal pressures up to 42 MPa are imposed to the FEM model. Although the software considers the last value for higher normal pressures, the contact shear stress during the simulation is logically limited to the shear strength of the material, just similar to the pin-on-disk experiments.

3.2 Flow stress

The tensile test of the annealed copper and aluminum can only give flow stress of the material at strains below 0.3–0.4 (before necking). However, material in tube-spinning process undergoes strains much more than these values, especially at high thickness reductions. To simulate the process by FEM analysis, therefore, it is necessary to measure flow stress of the material at high strains. To do this, two specimens were processed at 30% and 50% thickness reductions, while no bonding occurred due to the lack of proper surface treatment. Therefore, it was possible to prepare tensile specimens from the processed layers of copper and aluminum. The yield stress of these specimens was used as their flow stress at the strains induced in thickness reductions of 30% and 50%. FEM analyses were used to calculate the related strains. These FEM analyses were carried out at two steps: first by the flow stress obtained from the tensile test of the annealed specimens (work hardening up to 0.3–0.4 strains, and constant stress thereafter) and then by including the measured yield stress of the processed specimens at strains obtained from the previous step. The resulted average of equivalent plastic strain distribution through the thickness of the copper and aluminum layers were considered as the strains relating to the processed specimens. The results are illustrated in Fig. 8. These curves were imposed in the subsequent FEM models.

4 Results and discussions

4.1 Fractography

Among proposed bonding mechanisms, film theory is accepted as the major mechanism of cold and warm bonding processes such as roll bonding [5, 16]. This theory states that two opposing oxide layers break up during deformation and underlying virgin metal extrudes under the action of normal pressure through widening cracks in the surface layers and then, bond spots form on the overlapped regions of extruded virgin metals of two layers [5, 17]. This mechanism has been confirmed by SEM study of the fractured bond surfaces [5, 17–19]. Because of low temperature and short time of pressure applying on the layers in the tube-spinning process, film theory is considered as the major mechanism of spin bonding.

Figure 9 illustrates the SEM micrograph of the scratch brushed surfaces of copper and aluminum tubes after degreasing and before spin bonding. Based on the film theory scratch brushing provides rough surfaces with greater amount of surface asperities and promote a localized shear deformation that breaks unavoidable surface oxide films during deformation, contributing to the bonding of two metals [20]. Figure 9 shows that the surface layer is highly deformed in the wire brushing direction and some asperities and cracks are formed. However, because of higher strength and more work hardening of copper compared with aluminum, deformation occurred on the copper surface is slighter than the aluminum one.

SEM micrograph of the peel fracture surfaces of copper and aluminum spin bonded at room temperature with thickness reduction of 45% is illustrated in Fig. 10. Bright regions of this figure are bonded regions which had necked

Table 2 The parameters of pin-on-disk test

Parameter	Value
Pin diameter	4 mm
Pin head radius	3 mm
Disk diameter	26 mm
Sliding speed	4 mm/s

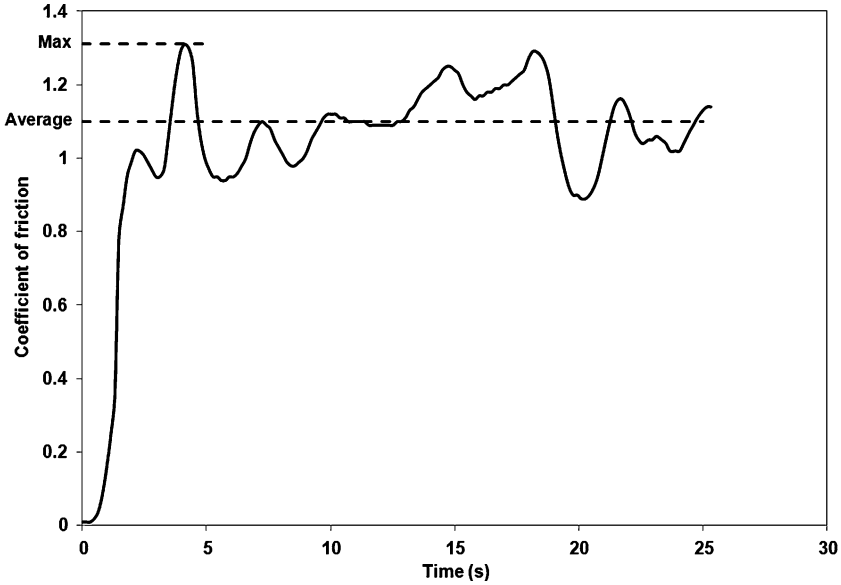

Fig. 5 Recorded coefficient of friction during the pin-on-disk test for normal load of 1 kg

and fractured during the peel test. Considering the metal and oxide hardness, Table 3, Mohamed and Washburn [5] have stated that compared with quite brittle aluminum oxide, copper oxide is relatively ductile and to some extent would deform with the base metal. In this case, the oxide film brakes in a shear manner. This is proven in the crack patterns observed in their SEM fractographies. They observed that while surface cracks at the bonding of Al/Al propagate normal to the rolling direction (brittle fracture), discontinuities on the surface of the Cu/Cu bonding are in the form of steps and stria (fail in a shear manner). SEM micrographs of this work, Fig. 10, show a similar pattern on the copper at spin bonding of Cu/Al. It should be noted here that as a result of mentioned fracture manner of copper oxide film, the pattern of bonded regions in aluminum would be different with that of Al/Al bonding [13].

4.2 Effects of process parameters on the bond strength

4.2.1 Effect of thickness reduction

The effects of thickness reduction and process temperature on the bond strength of Cu/Al tubes are illustrated in Fig. 11. It can be seen in this figure that like roll bonding, the bond is not created at thickness reductions less than a threshold value. Based on this figure, the threshold thickness reduction for spin bonding of these two metals is about 30%. In this process, unlike the rolling in which

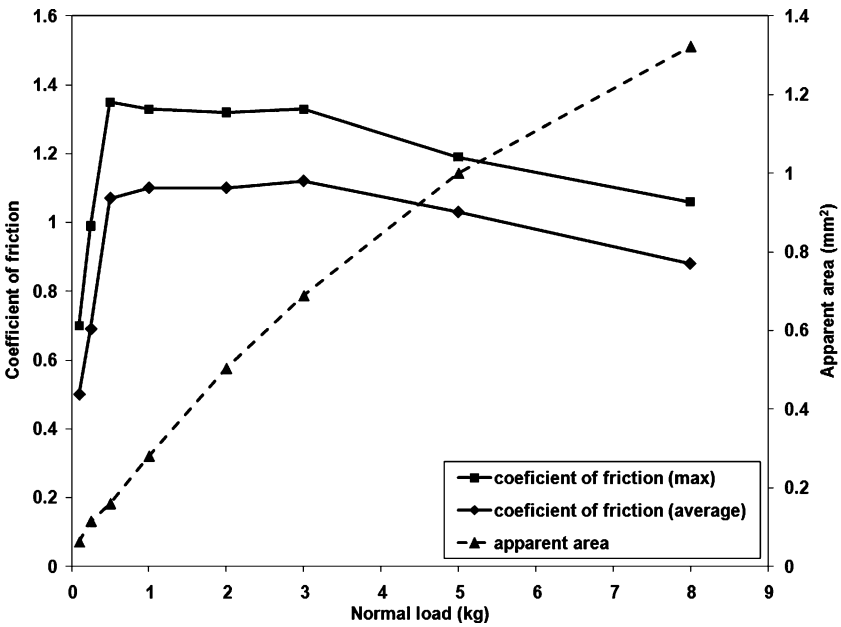

Fig. 6 Coefficient of friction and the apparent area measured at various normal loads

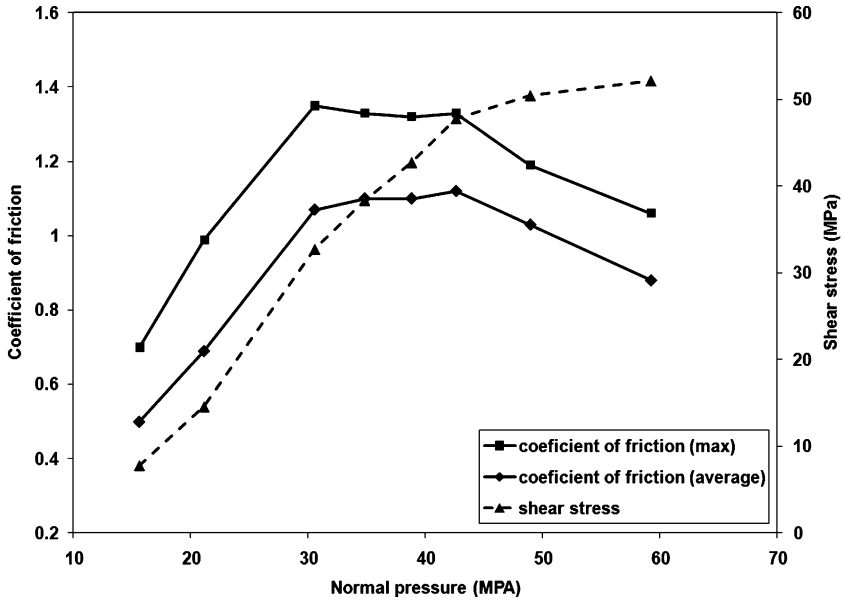

Fig. 7 Coefficient of friction and the shear stress at various normal pressures

deformation occurs in a simple symmetric plane strain conditions, deformation is more complicated and consists of more components of strains. It is illustrated that all three shear strains exist in tube spinning [21]. On the other hand, as mentioned in section 4.1, the copper oxide film fractures in a shear manner. Therefore, it can be said that the stress and strain states of tube-spinning process, especially shear strains, make it appropriate for spin bonding of Cu/Al.

Figure 11 shows that by increasing the thickness reduction after the threshold value, the bond strength increases. Based on the film theory, higher deformation leads to formation of more widening cracks and extrusion of more virgin metal to the interface. Therefore, area of overlapping virgin metal, i.e., the bond area, would increase, resulting in enhancement of the bond strength [5]. Mohebbi and Akbarzadeh [13] have presented an analytical model to study the strain history of spin bonding, according to which the mechanism of spin bonding is explained in two stages: surface preparation before occurrence of a stable bond and bond strengthening thereafter. By increasing the thickness reduction the second stage of bonding (strengthening) lasts longer and so the bond strength is increased, as it is experimentally illustrated in Fig. 11.

4.2.2 Effect of process temperature

It can be seen in Fig. 11 that increase of process temperature from the room temperature to 230°C has a negative effect on the resulted bond strength. Previous work

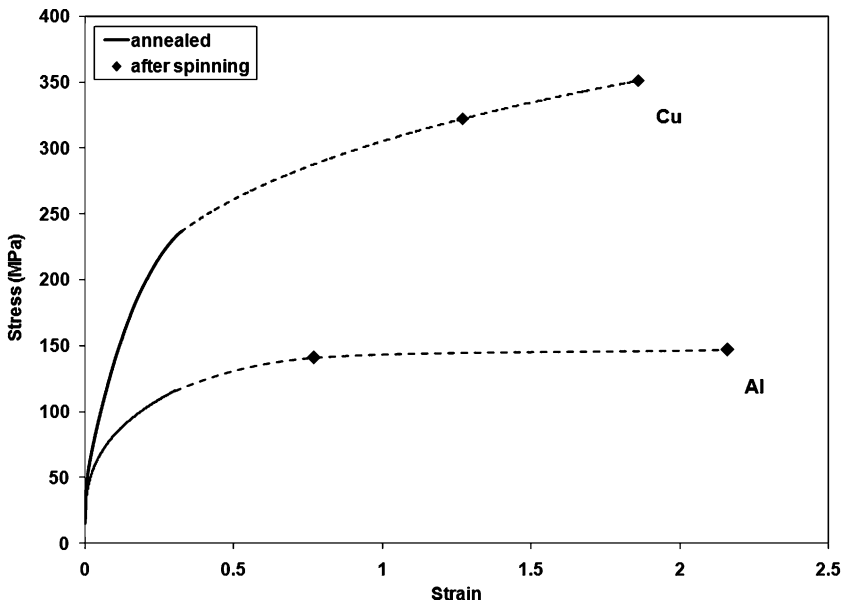

Fig. 8 Flow stress of the copper and aluminum used in the FEM analyses

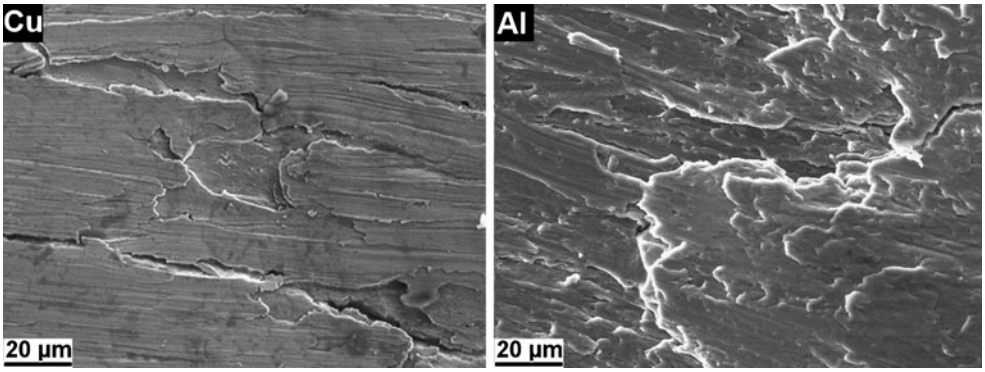

Fig. 9 SEM micrograph of the scratch brushed surface of copper and aluminum tubes

for roll bonding of Cu/Al at three temperatures of 350°C, 430°C, and 500°C by Peng et al. [1] shows optimum bond strength at 430°C. It is stated that enhancement of oxide formation on the metal surfaces which reduces physical contact area between the metals has a negative effect on roll bonding at high temperatures. Softening the material at high temperatures, on the other hand, results in formation of a stronger bond. Therefore, these opposite effects are considered as conditions for an optimum process temperature for roll bonding of Cu/Al [1]. The bond strengths obtained in their work for as rolled condition, however, are between 2.5 and 5 N/mm which are weak in comparison with the bond strength of the roll-bonded Cu/Al at room temperature (about 18 N/mm [2]). So, their conclusion about existence of an optimum temperature for roll bonding of Cu/Al is valid only for the specified range of temperature.

A major difference between roll bonding and spin bonding is the deformation history. While deformation in rolling occurs continuously from the initial thickness to the final one, in tube spinning, as an incremental forming process, deformation occurs at several steps of reduction, each of them happens in one revolution of the workpiece. The incremental nature of the process is well illustrated by Mohebbi and Akbarzadeh [21]. In other words, material is deformed in a very small portion of time at any revolution and is relaxed in remained time until the next revolution. Therefore, material experiences a repeated period of deformation and relaxation at the process temperature until reaching the final thickness. So, there is a considerable time for atoms to diffuse in spin bonding at high temperatures. This is more significant when considering the effects of deformation on the enhancement of atomic diffusion. The generation and migration of excess defects during deformation, short circuiting along static or moving dislocations or grain boundaries created by the deformation and short circuiting along cracks created during deformation are the ways that atomic diffusion is promoted [7]. Because of high affinity of copper and aluminum to each other, atomic diffusion in bonding of Cu/Al results in formation of intermetallic phases on the bond interface. This is observed in roll-bonded samples of Cu/Al annealed at high temperatures. The intermetallic compounds have a non-metallic covalence bond and therefore are brittle. So, the fracture of bonded interface is brittle due to presence of intermetallic phases, leading to lower bond strength [2, 4, 6]. Longitudinal section of the bond interfaces at three process temperatures are studied by chemical etching to examine the formation of intermetallic layer, Fig. 12. Clear dark and thick layer on the interface of specimen spin bonded at room temperature and annealed at 400°C for 30 min (Fig. 12a) confirms the capability of used etchant for darkening the intermetallic layer. It can be seen that no intermetallic layer forms at room temperature (Fig. 12b). At 130°C, however, a very thin intermetallic layer is formed at

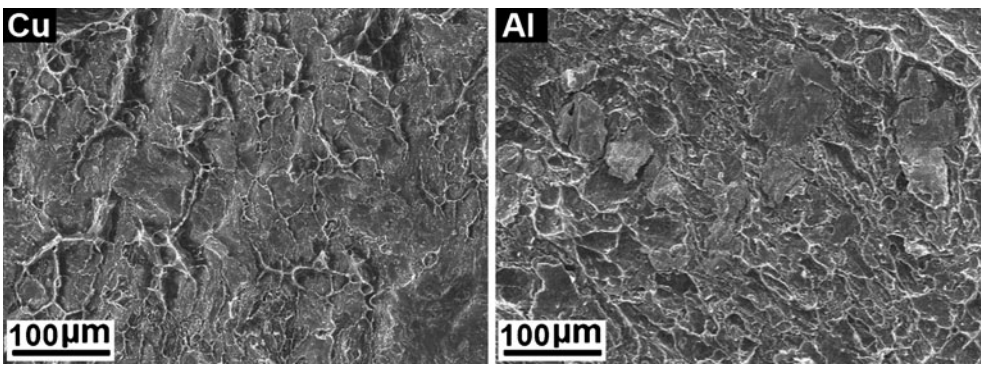

Fig. 10 SEM micrographs of the peel surfaces of copper and aluminum by spin-bonding of Cu/Al at 298 K and thickness reduction of 45%

Table 3 Hardness of copper, aluminum, and their oxides at room temperature [5]

Metal	Hardness (HV)	Oxide	Hardness (HV)
Cu	40	Cu_2O	160
Al	15	Al_2O_3	1,800

the interface (Fig. 12c). It can be seen also that an apparent and continuous intermetallic layer is formed on the interface of specimen spin bonded at 230°C (Fig. 12d). Based on this figure, it can be said that decrease of the bond strength by increasing the process temperature illustrated in Fig. 12 is related to the formation of brittle intermetallic layers on the bond interface at high temperatures.

5 Bonding model

In this section, a simple model for the bond strength which considers special aspects of the bonding mechanism in spin bonding is proposed.

5.1 Indirect calculation of the bonding length

All conditions of the experimental work are imposed to the FEM model except that the bonding is not considered. A model is developed here to calculate the bonding length by comparison of thickness ratio obtained from the simulations and the experiments. The basic point is that bonding as a constraint on the contact surfaces would affect the final thickness ratio of external tube to the internal one. Here, it is explained that in spite of such a high coefficient of friction depicted in Fig. 7, how two layers move against each other before bonding. In fact, based on Fig. 7, the pressure in which the frictional shear stress reaches to the shear strength of the material (and therefore no sliding is occurred between the two layers) is too low in comparison with the pressures applied during deformation. Therefore, it can be assumed that during deformation no sliding would occur. However, due to incremental nature of the process, any point of the contact surface undergoes a periodic pressure, from the maximum value under the roller to zero when it is released from the roller pressure. It is obvious that during this periodic variation of pressure, two surfaces would have some relative sliding under the influence of shear stresses.

It is considered in the present model that when two layers are bonded, their displacement and therefore their increment of the strain at the axial direction are the same, $d\varepsilon_{z_e} = d\varepsilon_{z_i}$. That is due to lack of relative sliding after bonding. Regarding the constancy of the diameters of tubes which leads to $d\varepsilon_\theta = 0$, it is concluded that after bonding the radial strain increments of the internal and the external layers would be the same:

$$d\varepsilon_{r_e} = d\varepsilon_{r_i} \tag{1}$$

Integration of this equation with attention to $d\varepsilon_r = \frac{dT}{T}$ leads to the constancy of the thickness ratio after the bonding:

$$\frac{T_{e_f}}{T_{i_f}} = \frac{T_e}{T_i} = \frac{T_{e_b}}{T_{i_b}} \tag{2}$$

The constancy of thickness ratio after the bonding was previously proposed by Hwang et al. [22] in their study of roll bonding.

Since the bonding is not considered in the FEM analyses, Eq. 2 is not satisfied in the simulation model. The results of these simulations showed that due to lower strength and work hardening of aluminum, the rate of thickness reduction in the internal layer is higher than that of the external one (copper). In the present model, the rate

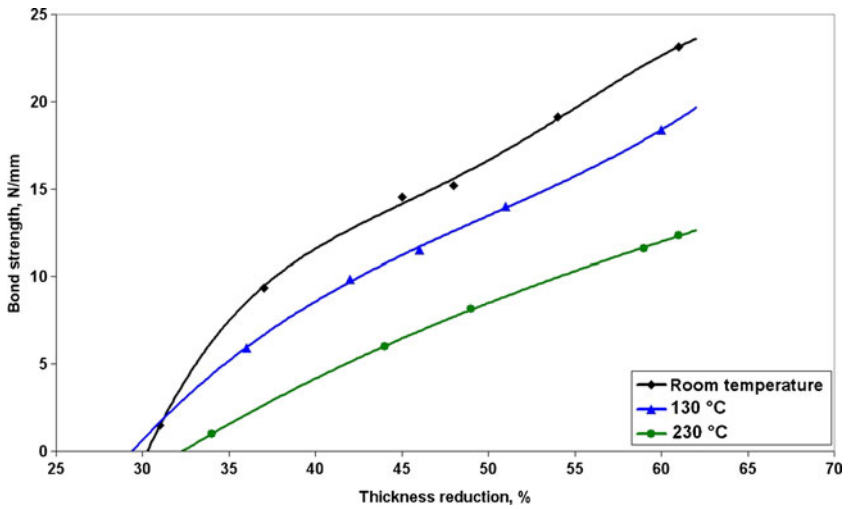

Fig. 11 The bond strength of Cu/Al tubes versus thickness reduction at various spin-bonding temperatures

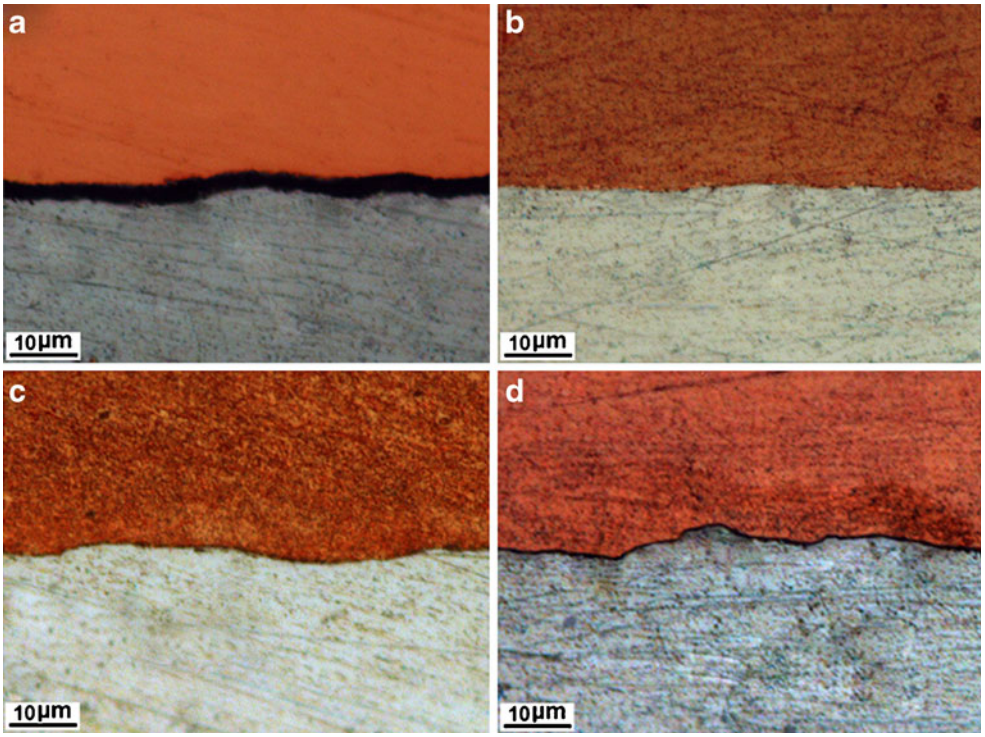

Fig. 12 Longitudinal section of the bond interfaces after chemical etching. Specimens are spin bonded at thickness reduction of 60% and temperatures of **a** 298 K and annealed at 673 K for 30 min, **b** 298, **c** 400, and **d** 500 K

of thickness reduction at deformation zone is simplified to be linear. Figure 13 illustrates a schematic comparison of the thickness reduction of two layers at the longitudinal section of tubes, with (by Eq. 2) and without (by FEM simulation) considering the bonding. By means of the geometry illustrated in this figure, it is possible to calculate indirectly the bonding length, l_b, from the T_{if} (experiment) and T'_{if} (FEM simulation) as below.

From the lower dash line the thickness of the internal layer at bonding section is:

$$T_{i_b} = T'_{if} + \left(\frac{T_{i_0} - T'_{if}}{L}\right) l_b \tag{3}$$

in which the axial length of deformation zone, L is:

$$L = \frac{T_0 - T_f}{\tan\alpha} = \frac{r\,T_0}{\tan\alpha} \tag{4}$$

The thickness at bonding section can also be calculated from the upper dash line (developed from Eq. 2):

$$T_{i_b} = T_{i_f} + \left(\frac{T_{i_f}}{(1-r)T_0}\tan\,\alpha\right) l_b \tag{5}$$

Considering Eqs. 3–5, the bonding length is calculated as below:

$$l_b = \frac{r\,(1-r)\,T_0\,\left(T_{i_f} - T'_{i_f}\right)}{\tan\alpha\,\left[(1-r)\,\left(T_{i_0} - T'_{i_f}\right) - r\,T_{i_f}\right]} \tag{6}$$

The final thickness of tubes are measured directly from the longitudinal sections after various thickness reductions for both FEM simulations and the experimental specimens. Figure 14, for example, shows the longitudinal section of tubes after thickness reduction of 37%. It is necessary to note that the calculated bonding length is highly sensitive to the precision of the thickness measurement. While in this work the average thicknesses of both simulations and experiments are measured with precision of 0.001 mm, the variation of final thicknesses were in the range of 0.020 mm. The results are summarized in Table 4. Figure 15 shows the bonding length as a function of the thickness reduction.

5.2 The bond strength

Mohamed and Washburn [5] have presented a theoretical calculation of the bond strength at cold bonding. This theoretical model is developed here for spin bonding. Based on this theory, bonding is assumed to occur whenever

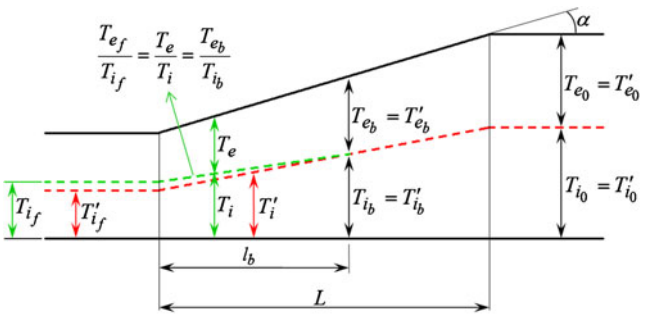

Fig. 13 Schematic longitudinal section of the tubes demonstrating the geometric components of the model

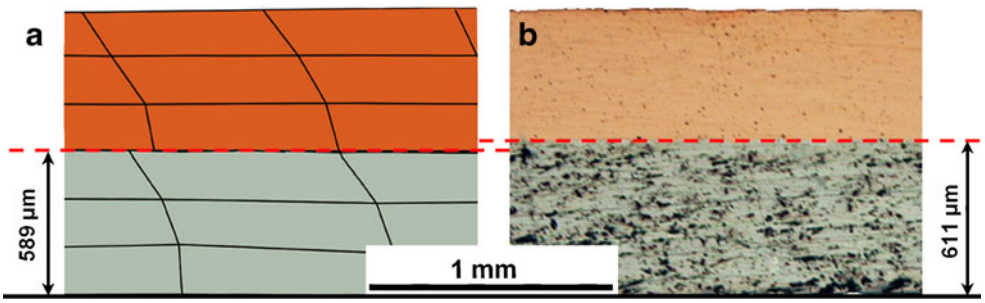

Fig. 14 Longitudinal section after thickness reduction of 37%; **a** FEM simulation and **b** experiment

virgin metals come into contact (correlation contact of virgin metals). The virgin metallic area of each layer, on the other hand, is proportional to the amount of surface extension. With regard to $A = \pi Dl$ and $Tl = \text{cte}$ (volume constancy), the amount of surface fraction of virgin metal is given by:

$$f_A \propto \frac{A - A_0}{A} = \left(1 - \frac{l_0}{l}\right) = \left(1 - \frac{T}{T_0}\right) = r \tag{7}$$

In spin bonding, the thickness reduction (and therefore the surface extension) is divided into two parts: before the bonding section (r_b) and thereafter ($r - r_b$). It is assumed that these two parts contribute in bonding following two distinct functions.

At first, the contribution of surface extension after bonding is explained. At an extreme state, if cracks in oxide films nucleate and grow quite independent at two surfaces, the surface fraction of correlated contact of virgin metals, f_{A_c}, would be proportional to the multiplication of the surface extensions of two layers (the square of thickness reduction). Another extreme, on the other hand, is when the cracks of two surfaces form completely in consistent with each other. In this case, the fraction of correlated contact of virgin metals would be proportional to the surface extension which is equal to thickness reduction (according to Eq. 7). After the bonding section, no relative sliding occurs and therefore it is reasonable to consider a mixed state:

$$f_{A_c}{}^{I} \propto (r - r_b)^n, \quad 1 < n < 2 \tag{8}$$

where r_b is given by:

$$r_b = r - \frac{\tan\alpha}{T_0} l_b \tag{9}$$

Table 4 Results of thickness measurement and calculation of the bonding length for T_{i0}=0.997 mm, T_0=1.821 mm, and α=17°

r (%)	T'_{if} (mm)	T_{if} (mm)	l_b (mm)
31	0.653	0.658	0.191
37	0.589	0.611	0.986
49	0.445	0.490	1.617
61	0.298	0.368	2.061

in which l_b is calculated from Eq. 6. The bond strength is proportional to the surface fraction of bond spots, i.e. the surface fraction of correlated contact of virgin metals. It can be written from Eqs. 8 and 9 that:

$$S_b{}^{I} = c_1 \left(\frac{\tan\alpha}{T_0} l_b\right)^n \tag{10}$$

Before the bonding section, there is some relative sliding between two layers. At this condition, it is assumed that the cracks form independently at two surfaces. The surface fraction of correlated contact of virgin metals, therefore, is proportional to the square of thickness reduction before the bonding section:

$$f_{A_c}{}^{II} \propto r_b{}^2 \tag{11}$$

Virgin metals exposed to the surface before the bonding section have a potential for bonding. This potential, however, does not create a bond until it begins at the bonding section. Thereafter, those virgin metals can contribute to bonding in addition to virgin metals exposed after the bonding section. This contribution does not occur suddenly after the bonding section, but it occurs gradually by increasing the thickness reduction from that of the bonding section. Simply, this gradual contribution is assumed to occur linearly after the bonding section. Therefore, the relevant bond strength is given by:

$$S_b{}^{II} = c_2 r_b{}^2 (r - r_b) \tag{12}$$

Substituting r_b from Eq. 9, this portion of the bond strength is:

$$S_b{}^{II} = c_2 \left(r - \frac{\tan\alpha}{T_0} l_b\right)^2 \left(\frac{\tan\alpha}{T_0}\right) l_b \tag{13}$$

The final bond strength is obtained from the summation of two portions, Eqs. 10 and 13:

$$S_b = c_1 \left(\frac{\tan\alpha}{T_0} l_b\right)^n + c_2 \left(r - \frac{\tan\alpha}{T_0} l_b\right)^2 \left(\frac{\tan\alpha}{T_0}\right) l_b \tag{14a}$$

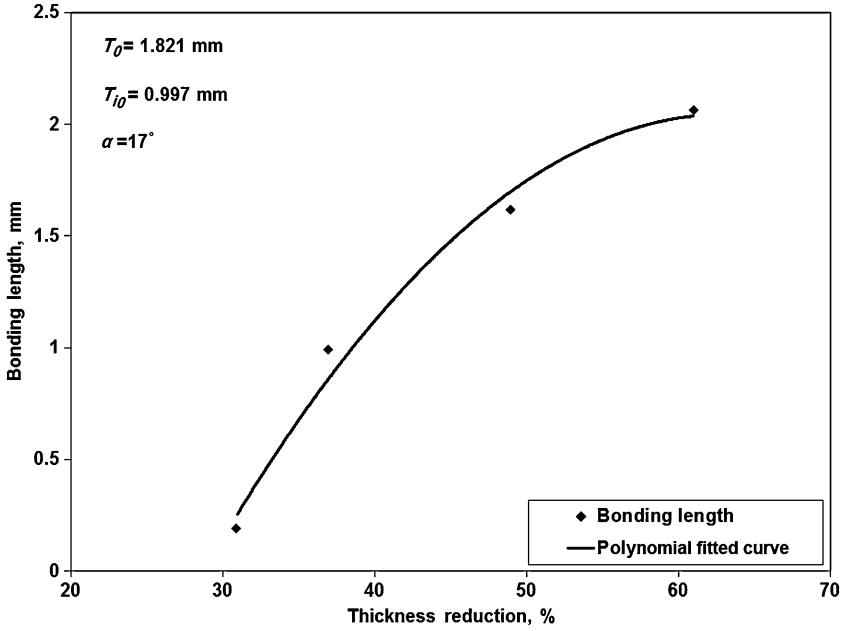

Fig. 15 Bonding length calculated from Eq. 6 at various thickness reductions

Substituting tan α and T_0 into constants, the following equation is obtained:

$$S_b = c_1' l_b{}^n + c_2' \left(r - \frac{\tan\alpha}{T_0} l_b \right)^2 l_b \tag{14b}$$

Since l_b is calculated in section 5.1 as a function of r (Fig. 15), Eqs. 14a and 14b gives a relation between the bond strength S_b and the thickness reduction r. The constants c_1 and c_2 depend on the surface treatment and process parameters. The exponent, n is related to how independent the cracks are formed on surfaces after the bond section. It is necessary to make the point that although α and T_0 are contributed in Eqs. 14a and 14b, this equation does not show their effects on the bond strength, because c_1 and c_2 depend also on these parameters.

Fitting to the existing experiments at room temperature (Fig. 11) and calculated bonding length (Fig. 15), the parameters in Eqs. 14a and 14b are obtained. The resulted graph and its accordance with the experiments are plotted in Fig. 16. It can be seen that the model can well cover the inflection point in trend of bond strength at 45% thickness reduction. Regarding the contribution of two portions by Eqs. 10 and 13 which are depicted in Fig. 16, the increasing rate of bond strength after thickness reduction of 45% is mostly due to the S_b^{II} (bond strength caused by extrusion of virgin metals before the bonding section). In fact, S_b^{II} has a

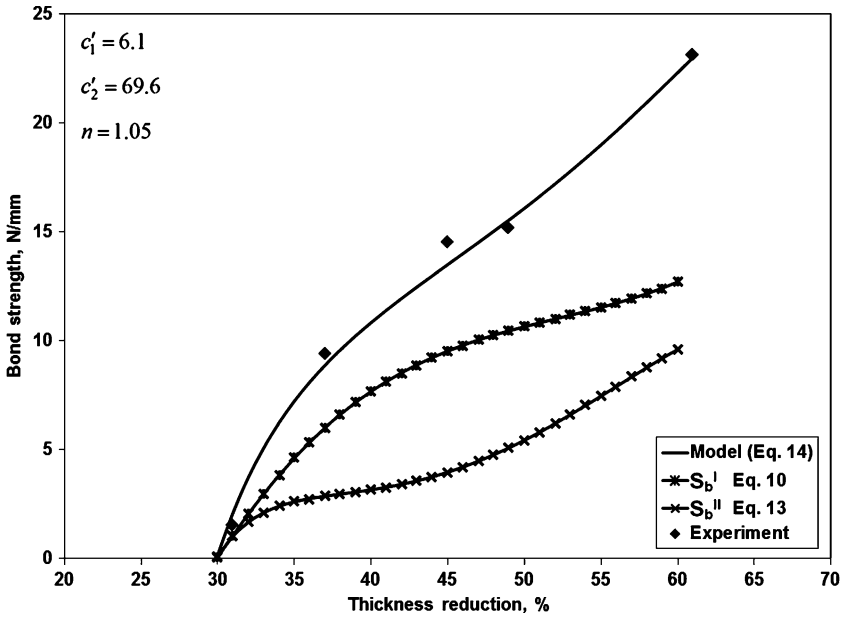

Fig. 16 The bond strength versus the thickness reduction from the experiments and the modeling

little contribution to the bond strength before 45% thickness reduction and its contribution increases rapidly thereafter. This trend arises from the fact that increase of bonding length (l_b) is slow after the mentioned thickness reduction (Fig. 15), while the axial length of the deformation zone (L) increases monotonically. Therefore, L-l_b (the length of section in which virgin metal is extruded to the surface and makes a potential for S_b^{II}) increases.

6 Conclusions

Copper and aluminum tubes were bonded by the spin-bonding process to produce a two layers clad tube. Evaluation of the bond quality at various thickness reductions and process temperatures leads to the following conclusions:

1. The threshold thickness reduction for spin bonding of Cu/Al is about 30%. Similar to other cold and warm bonding processes, the bond strength is increased by deformation after this threshold value.
2. The SEM micrograph of the peel surface of copper illustrates that fracture of the oxide film occurs in a shear manner. These shears are intensified by shear stress and strains applied during spin bonding, making it appropriate to bonding of the copper tube.
3. Increasing the process temperature leads to the reduction of the bond strength. It is shown that the brittle intermetallic layer formed at high temperatures is the main cause of this reduction.
4. By comparison of the FEM simulations, which do not consider the bonding constraint, with the experiments, a procedure is proposed and used for indirect calculation of the bonding length.
5. Based on the calculations of bonding length and the bonding mechanism, a model for the bond strength at spin bonding is developed in which the bond strength is contributed to two distinguished parts of before and after bonding section.

References

1. Peng XK, Heness G, Yeung WY (1999) Effect of rolling temperature on interface and bond strength development of roll bonded copper/aluminium metal laminates. J Mater Sci 34:277–281
2. Abbasi M, Taheri AK, Salehi MT (2001) Growth rate of intermetallic compounds in Al/Cu bimetal produced by cold roll welding process. J Alloys Compd 319:233–241
3. Zhan Z et al (2006) Cladding inner surface of steel tubes with Al foils by ball attrition and heat treatment. Surf Coat Technol 201:2684–2689
4. Heness G, Wuhrer R, Yeung WY (2008) Interfacial strength development of roll-bonded aluminium/copper metal laminates. Mater Sci Eng A 483–484:740–742
5. Mohamed HA, Washburn J (1975) Mechanism of solid state pressure welding. Weld J 54:302s–310s
6. Peng XK et al (1999) On the interface development and fracture behaviour of roll bonded copper/aluminium metal laminates. J Mater Sci 34:2029–2038
7. Peng XK (2000) Rolling strain effects on the interlaminar properties of roll bonded copper/aluminium metal laminates. J Mater Sci 35:4357–4363
8. Lee JE et al (2007) Effects of annealing on the mechanical and interface properties of stainless steel/aluminum/copper clad-metal sheets. J Mater Process Technol 187–188:546–549
9. Chen Z et al (2003) Fabrication of composite pipes by multi-billet extrusion technique. J Mater Process Technol 137:10–16
10. Sponseller DL, Timmons GA, Bakker WT (1998) Development of clad boiler tubes extruded from bimetallic centrifugal castings. J Mater Eng Perform 7:227–238
11. Berski S et al (2006) Analysis of quality of bimetallic rod after extrusion process. J Mater Process Technol 177:582–586
12. Wang X, Lib P, Wang R (2005) Study on hydro-forming technology of manufacturing bimetallic CRA-lined pipe. Int J Mach Tools Manuf 45:373–378
13. Mohebbi MS, Akbarzadeh A (2010) A novel spin-bonding process for manufacturing multilayered clad tubes. J Mater Process Technol 210:510–517
14. Wong CC, Dean TA, Lin J (2003) A review of spinning, shear forming and flow forming processes. Int J Mach Tools Manuf 43:1419–1435
15. Wong CC, Dean TA, Lin J (2004) Incremental forming of solid cylindrical components using flow forming principles. J Mater Process Technol 153–154:60–66
16. Vaidyanath LR, Nicholas MG, Milner DR (1959) Pressure welding by rolling. Br Weld J 6:13–28
17. Cave JA, Williams JD (1975) The mechanisms of cold pressure welding by rolling. J Inst Met 101:203–207
18. Bay N (1986) Cold welding: Part I. Characteristic, bonding mechanisms, bond strength. Met Constr 18:369–372
19. Wright PK, Snow DA, Tay CK (1978) Interfacial conditions and bond strength in cold pressure welding by rolling. Met Technol 1:24–31
20. Li L, Nagai K, Yin F (2008) Progress in cold roll bonding of metals. Sci Technol Adv Mater 9:1–12
21. Mohebbi MS, Akbarzadeh A (2010) Experimental study and FEM analysis of redundant strains in flow forming of tubes. J Mater Process Technol 210:389–395
22. Hwang YM, Hsu HH, Hwang YL (2000) Analytical and experimental study on bonding behavior at the roll gap during complex rolling of sandwich sheets. Int J Mech Sci 42:2417–2437